Letter to the Editor

Aggressive primary thyroid lymphoma invading the internal jugular vein: a case series

Xuejiao Su[1], Xue Hu[2], Buyun Ma[1]

[1]Department of Medical Ultrasound, West China Hospital of Sichuan University, Chengdu, China; [2]Department of Pathology, West China Hospital of Sichuan University, Chengdu, China

Correspondence to: Buyun Ma. Department of Medical Ultrasound, West China Hospital of Sichuan University, 37 Guoxue Alley, Chengdu 610041, China. Email: mabuyundoctor@163.com.

Submitted Jun 21, 2022. Accepted for publication Oct 30, 2022. Published online Nov 10, 2022.
doi: 10.21037/qims-22-649
View this article at: https://dx.doi.org/10.21037/qims-22-649

Introduction

Primary thyroid lymphoma (PTL) is a rare malignant disease originating from the thyroid. Its incidence is less than 5% of all malignant thyroid diseases, and less than 2% are extra-nodal lymphoma (1). PTL is most often characterized by a rapidly growing neck lump in a short period of time as the first symptom. The literature on PTL involving adjacent tissues is relatively rare, and the literature on the invasion of the internal jugular vein is even more rare. The available literature most often reports on the encirclement of the internal jugular vein, with little direct evidence of the invasion of the lumen (2-4). We report on 3 cases of aggressive PTL, all of which invaded the internal jugular vein, and a tumor thrombus formed. The pathological type of all 3 cases was diffuse large B-cell lymphoma (DLBCL). Contrast-enhanced ultrasonography (CEUS) was performed in all cases. The internal jugular vein thrombus in case 3 was confirmed to be a tumor thrombus by ultrasound-guided fine-needle aspiration biopsy (FNAB). To our knowledge, this is the first report of PTL invading the internal jugular vein with a tumor thrombus confirmed by an ultrasound-guided pathological puncture. We present the features of conventional ultrasound (US) and CEUS for PTL invasion of the internal jugular vein. Further, this study demonstrates that chemotherapy can also be used to treat an internal jugular vein tumor thrombus caused by PTL.

Case presentation

All procedures performed in this study were in accordance with the ethical standards of the Ethics Committee of West China Hospital and with the Helsinki Declaration (as revised in 2013). Written informed consent was provided by the patients for the publication of this case report and accompanying images. A copy of the written consent is available for review by the editorial office of this journal.

Case 1

A 79-year-old female was admitted to our hospital in December 2018 due to a neck mass and pain. She had an elevated thyroglobulin (Tg) level—Tg was 1,242.00 μg/L (normal range: 3.5–77 μg/L). A US performed in January 2019 revealed several marked hypoechoic nodules in the left lobe of the thyroid. The larger one was located in the upper part with a size of about 42 mm × 19 mm × 31 mm. The right lobe of the thyroid was almost occupied by a very low-echo nodule with a size of about 116 mm × 94 mm × 50 mm. The US of these nodules showed that they were heterogeneous hypoechoic masses with ill-defined margins, and they were wider than they were long. These nodules did not contain calcifications, liquefaction, posterior acoustic enhancement (PAE), or a peripheral hypoechoic halo. Color Doppler ultrasound (CDU) of these nodules revealed short strips of blood flow signals, and they were classified as grade 2 according to Adler grade classifications (5). The lymph nodes in the right cervical zones III and IV were enlarged. These thyroid nodules were classified as Thyroid Imaging Reporting and Data Systems (TIRADS) 5 according to the American College of Radiology (ACR-TIRADS) (6). Hypoechoic filling was detected in the

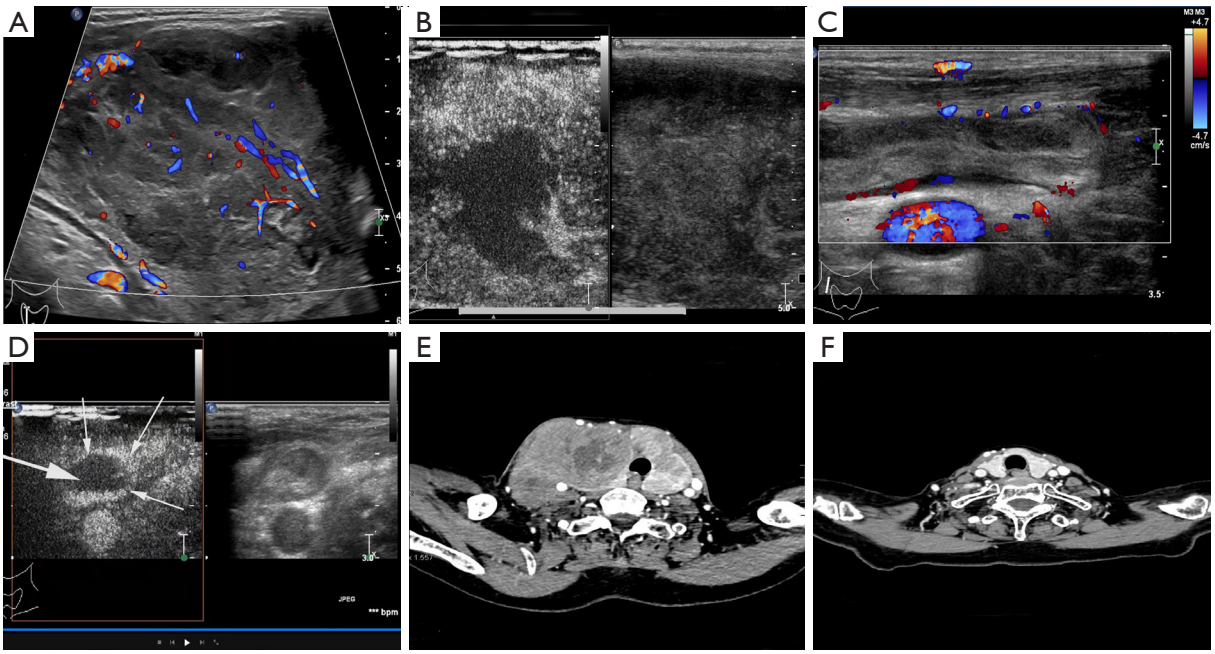

Figure 1 US, CEUS, and enhanced CT images of the neck in case 1. (A) A longitudinal image of US of the right thyroid gland shows an 11cm, irregular shaped, heterogeneous hypoechoic mass, replacing the entire right lobe of the thyroid, with dotted line-like blood flow signals. (B) For this mass, the contrast agent entered in a centripetal way and presented as hypo-enhancement and was heterogeneous. (C) The right internal jugular vein was filled with weak echoes, and some of the blood flow signals in the lumen were filled with defects. (D) CEUS shows that the internal jugular vein emboli presented no enhancement (thick arrow) in the central area but partial enhancement in the periphery (thin arrows). (E) Contrast-enhanced axial scan of the neck on CT revealed heterogenous soft tissue opacities occupying the bilateral thyroid lobes and isthmus, compressing the trachea and causing tracheal stenosis (January 2019). (F) CT shows that the thyroid lymphoma went into complete remission following treatment with chemotherapy (June 2022). US, ultrasound; CEUS, contrast-enhanced ultrasonography; CT, computed tomography.

lumen of the right internal jugular vein (RIJV). For these thyroid nodules, the contrast agent entered in a centripetal way and presented as heterogeneous hypo-enhancement. A CEUS of this RIJV embolus showed no enhancement in the center of the embolus but partial enhancement in the periphery, which suggested the possibility of the formation of RIJV thrombosis and tumor thrombus. Thrombosis is avascular and is not enhanced after contrast injection, whereas tumor thrombus involves malignant vascularity that is enhanced after the contrast agent enters microcirculation. In January 2019, contrast-enhanced CT of the neck revealed a mass of soft tissue density shadow at the bilateral thyroid lobes and isthmus with heterogeneous enhancement. The CT images showed a filling defect occluding the lumen of RIJV, and there was a mass compressing the trachea and narrowing of the tracheal lumen. FNAB and US-guided core needle biopsy (CNB) (18G) were performed for bilateral thyroid nodules. Immunohistochemistry (IHC) staining showed lymphocytic hyperplasia, mainly medium to medium-to-large lymphocytes, and plasma cells with CD20 (+), CD79a (+), CD3 (–), CD10 (–), BCL-6 (+, 30%), mum-1 (+), BCL-2 (+, 70–80%), C-MYC (–, 10–20%), and Ki-67 (+, >80%). Gene rearrangement showed low amplification peaks of IgH and IgK. Flow cytometry detected abnormally expressed B lymphocytes. Combined with the above results, the diagnosis was considered DLBCL with high proliferative activity (*Figure 1A-1F*).

The patient was treated with the R-CHOP (rituximab plus cyclophosphamide, doxorubicin, vincristine, and prednisone) regimen. After 4 months (May 2019), the enhanced CT of the neck was reviewed. Compared with the previous time, the mass was significantly smaller, and the thrombus was partially absorbed. A positron emission tomography-computed tomography (PET-CT) examination was performed in November 2021. After chemotherapy, the patient showed no signs of tumor recurrence throughout

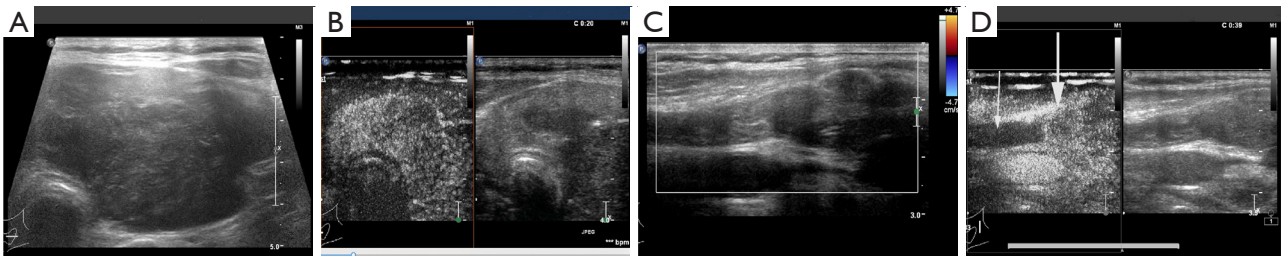

Figure 2 US and CEUS images of the thyroid and internal jugular vein tumor thrombus in case 2. (A) The transverse image of ultrasonography of the left thyroid gland showed a 7.8 cm, irregular-shaped, heterogeneous hypoechoic mass. (B) CEUS shows that the thyroid nodules presented low enhancement, heterogeneous enhancement, and concentric enhancement. (C) Color Doppler images of the LIJV. The LIJV was thickened, and hypoechoic mass filling was detected in the lumen. (D) LIJV angiography, the thickened segment of the left internal jugular vein showed heterogeneously high enhancement (thick arrow). Above the thickened segment, no enhancement (thin arrows) was shown. US, ultrasound; CEUS, contrast-enhanced ultrasonography; LIJV, left internal jugular vein.

their body. In June 2022, the contrast-enhanced CT images of the neck of the patient demonstrated that the thyroid lymphoma was indeed in complete remission (CR) after she received chemotherapy. In contrast to before treatment, the patient's RIJV tumor thrombus shrunk significantly, but there might have been some necrotic tissue remaining. The cervical and supraclavicular lymph nodes were not enlarged on CT images.

Case 2

An 89-year-old female was admitted to West China Hospital in September 2019 because of a lump in her neck. The patient's thyroid function was normal. An US examination showed that the reduced echogenicity of the thyroid parenchyma was heterogeneous. A hypoechoic nodule with a size of 78 mm × 40 mm × 75 mm was found in the left lobe, the isthmus, and the right lower lobe of the thyroid, with a shape that was wider than it was long, with a well-defined margin. Its internal echo was heterogeneous. No calcification, liquefaction, peripheral hypoechoic halo, or PAE was detected in this nodule. The patient's thyroid capsule was involved. A CDU showed that the Adler blood supply grading of this nodule was 1, and the arterial spectrum could be detected inside. Peak systolic velocity (PSV) was 25.1 cm/s, end diastolic velocity (EDV) was 3.35 cm/s, and the resistive index (RI) was 0.87. Lymph node enlargement was observed in the left cervical zone III. This thyroid nodule was classified as TIRADS 5 according to ACR-TIRADS classification. The left internal jugular vein (LIJV) was thickened, with a maximum inner diameter of about 22 mm, and hypoechoic filling was detected in part of the lumen. Dot-line blood flow signals were detected in the lumen of the thickened segment of the LIJV. For these thyroid nodules, the contrast agent entered in a centripetal way and presented with hypo-enhancement and heterogeneity. After injection of the contrast agent, the thickened segment of the LIJV showed heterogeneous hyperenhancement, and there was no enhancement above the thickened segment, which suggested tumor thrombus formation (*Figure 2A-2D*). The contrast agent could not pass through the LIJV blocked by the tumor thrombus, and there was no enhancement above the thickened vessel. Thyroid nodules underwent US-guided FNAB and CNB. The pathological findings showed large cells with irregular nuclear contours, vesicular chromatin, and several nucleoli. After IHC staining, the majority of these neoplastic cells were positive for CD20, Ki67 (+, ~50%), a small amount of CD3 (+) cells in the background, CD30 (–), CK (–), CD34 (–), STAT6 (–), Desmin (–), SMA (–), S-100 (–), EMA (–), and β-C (–), which indicated B-cell tumors. Due to the patient's old age, she and her family decided to delay treatment, which meant that this patient was considered lost to follow-up.

Case 3

A 79-year-old male was admitted to our hospital in August 2020 with a mass in his neck. His thyroid function tests were normal. His US showed hypoechoic and heterogenous thyroid parenchyma. There were multiple hypoechoic nodules in the thyroid. The size of the larger nodule on the right was about 82 mm × 58 mm × 41 mm, and the size of the larger nodule on the left was about 23 mm × 12 mm × 10 mm. These nodules were wider than they were

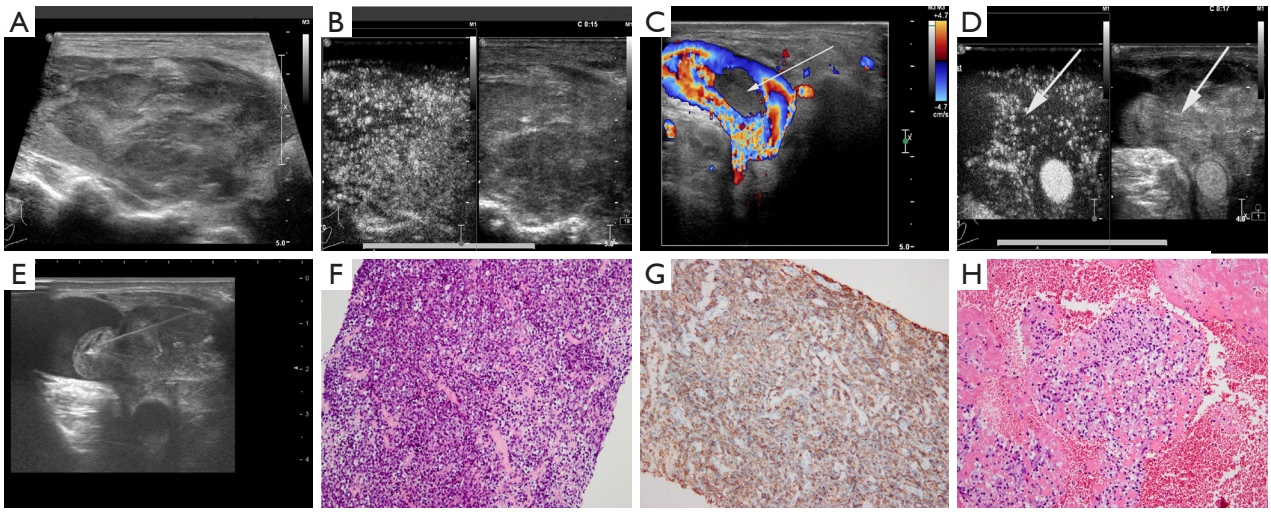

Figure 3 US, CEUS, and pathology images of thyroid nodules and RIJV tumor thrombus in case 3. (A) The longitudinal sonogram of the left lobe showed heterogeneous hypo-echogenicity with posterior acoustic enhancement. (B) CEUS showed that the thyroid nodules presented low enhancement, heterogeneous enhancement, and concentric enhancement. (C) An isoechoic mass (arrow) filling was found in the lumen of the right internal jugular vein, and a blood flow signal filling defect was observed. (D) The CEUS image revealed hypo-enhanced emboli (arrows) of RIJV with centripetal heterogeneity. (E) Ultrasound-guided FNAB of the right internal jugular vein tumor thrombus. (F) Pathological examination of the thyroid nodule showed diffuse proliferation of moderately large atypical lymphoid cells (HE staining, ×200). (G) Atypical lymphoid cells showed expression of CD20 (CD20 immunostaining, ×200). (H) A small amount of atypical lymphoid cells that were large and had irregular nuclear contours, vesicular chromatin, and one or more nucleoli were found under the pathological microscope of the RIJV emboli (HE staining, ×200). US, ultrasound; CEUS, contrast-enhanced ultrasonography; RIJV, right internal jugular vein; FNAB, fine-needle aspiration biopsy; HE, hematoxylin and eosin.

long, with ill-defined margins, heterogeneous internal echogenicity, and PAE. No calcification, liquefaction, or peripheral hypoechoic halo was detected in any of them. The CDU showed that the Adler blood supply grading of these nodules was 2. The patient's thyroid capsule was involved, the nodule wrapped around the right common carotid artery, and there was no obvious abnormality in bilateral cervical lymph nodes. These thyroid nodules were classified as TIRADS 5 according to ACR-TIRADS classification. In the lumen of the RIJV, an isoechoic mass with a size of about 29 mm × 12 mm × 15 mm was detected. From the linear blood flow signal at the inner part of the mass, the arterial pulse spectrum was detected, and PSV was 30.9 cm/s, EDV was 6.01 cm/s, and RI was 0.81. For these thyroid nodules, the contrast agent entered in a centripetal way and presented with hypo-enhancement and heterogeneity. As for CEUS, the emboli presented as hypo-enhanced, with a centripetal heterogeneous pattern. This suggested that the emboli were tumor thrombus. Under US guidance, CNB was performed for the right thyroid lobe nodules, and FNAB was performed for the RIJV emboli. The pathologic specimen from CNB revealed a diffuse proliferation of atypical intermediate to large atypical lymphoid cells. Immunophenotype detected follicular epithelial cells PCK (+) lymphocytes showed CD20 (+), CD3 (–), CD10 (+), BCL-6 (+), MUM-1 (+), BCL-2 (–), C-MYC (+, 70%), Ki-67/MIB-1 (+, >90%), CD79a (+), CD19 (+), and CD38 (+, few). Flow cytometry detected light chain-restricted expression of the B lymphocyte population. Gene rearrangement detection showed IgH and IgK clonal amplification peaks but no gamma T cell receptor (TCRG) clonal amplification peaks. Combined with the above results, the diagnosis was aggressive B-cell lymphoma, consistent with DLBCL, which was of germinal center B-cell origin (per Hans classification) and had high tumor cell proliferation activity. Pathological examination of the embolus revealed some swollen vascular endothelial cells and very few atypical lymphoid cells that were large and had irregular nuclear contours, vesicular chromatin, and one or more nucleoli (*Figure 3A-3H*). The patient received the R-CHOP regimen and achieved CR in June 2021.

Discussion

PTL is a rare malignant disease originating from the thyroid, with an incidence of less than 5% of thyroid malignancies and less than 2% of extra-nodal lymphoma (1). The most common feature of PTL is a neck mass that grows rapidly over a short period of time as the first symptom. Most pathological types of PTL are non-Hodgkin lymphoma derived from B cells, of which marginal zone lymphoma and DLBCL are the main types. DLBCL is more invasive than marginal zone lymphoma, and the 5-year survival rate of DLBCL is lower than that of marginal zone lymphoma. DLBCL is mainly treated with radiotherapy and chemotherapy, and marginal zone lymphoma is primarily treated with radiotherapy (7).

US is usually the initial modality for the diagnosis of thyroid lesions. The masses were shown to be heterogeneous and hypoechoic on US images in all 3 cases reported here. These hypoechoic areas corresponded to lymphoepithelial lesions of PTL (8). CEUS can assess the sequence, intensity, and hemodynamic characteristics of vascular perfusion in thyroid nodules, thereby providing a real-time characterization of the nodule following an intravenous bolus of microbubble contrast agent (9,10). Previous literature has reported that low enhancement, heterogeneous enhancement, and peripheral irregular enhancement patterns of thyroid nodules suggest malignancy (10-14). However, the diagnostic accuracy of malignant tumors can be improved by combing the internal enhancement pattern and the slow wash-in and wash-out curve that is slower than that of normal thyroid tissue.

CEUS also enables the distinction between thrombosis and tumor thrombus, such as malignant and non-malignant emboli in the portal vein, inferior vena cava, and renal veins (15,16). Thrombosis is avascular and does not enhance after the contrast injection, whereas tumor thrombus involves malignant vascularity that is enhanced after the contrast agent enters microcirculation. The no-perfusion area of the embolus may indicate thrombosis. Another possibility is that the tumor thrombus grows too fast, with the pathological basis that the tumor thrombus has no sufficient blood supply and is necrotic; therefore, the contrast agent does not enter the tumor thrombus. The emboli in case 1 showed peripheral enhancement, suggesting the possibility of tumor thrombus. There was no perfusion area in the middle part of the tumor thrombus, which could suggest necrosis. The tumor thrombus gradually shrank during chemotherapy. A frank thrombotic obstruction demonstrates no contrast enhancement, whereas a tumor thrombus shows enhancement of the obstructing filling material, as reported in case 2. Further, the contrast agent cannot pass through the LIJV blocked by the tumor thrombus; therefore, no enhancement is shown above the thickened vessel. The emboli of case 3 presented as hypo-enhanced with the centripetal heterogeneous pattern, which is similar to the enhancement pattern of thyroid lymphoma.

FNAB and CNB are common preoperative diagnostic tools for PTL. In contrast to surgery, they are less invasive (8,17,18). The initial diagnostic method for thyroid lymphoma should consist of FNAB with the use of additional techniques, such as the cell block technique, CNB, flow cytometry, and IHC staining for improved diagnostic accuracy (19,20).

PTL may invade adjacent structures around the thyroid, such as muscle, the esophagus, the trachea, and large vessels in the neck. There are only a few reports in the related imaging literature, and only one article has specified the invasion into the lumen of the RIJV. Hu *et al.* (3) reported DLBCL involving the RIJV and adjacent muscles. In this case, only image data from US and CDU were available, and no other preoperative data confirmed the nature of the embolus. The postoperative pathological diagnosis of the mass was DLBCL, and the surgery included thyroidectomy and resection of part of the RIJV and adjacent muscles. Compared to chemotherapy, surgery incurs more trauma and has the potential for complications. Kim *et al.* (2) reported cases in which the PTL lesions were closely adjacent to the LIJV and common carotid artery, but they did not clearly indicate the luminal interior of the invading vessel (*Table 1*).

This is the first report on the US and CEUS characteristics of PTL invading the internal jugular vein (IJV) with tumor thrombus formed. We report 3 cases of PTL invasion into the IJV. The patients had long history of Hashimoto's thyroiditis and presented with neck masses. The US features for the majority of previously reported PTL were homogeneous hypoechoic masses that rarely invaded adjacent structures (8). Our cases were quite different from these findings. The masses in our cases were shown to be heterogeneous and hypoechoic on US images in all 3 cases. This is similar to the aggressive PTL echogenicity already reported by Hu *et al.* (2,3). Echogenic heterogeneity of the lesion may be a feature of aggressive PTL. US images of case 3 showed that these masses had PAE. The masses of all cases were wider than they were tall, with echogenic strands and the absence of calcification and a peripheral halo. For the thyroid lesions in the above

Table 1 Summary of previous reported cases of PTL with invasion into adjacent structures

Series (references)	Age (years)/ sex	Clinical presentation	HT	Thyroid hormone levels	Diagnosis method	Structure of the invasion	Type of pathology	Stage of PTL	Treatment	Prognosis/ mortality
Kim *et al.* (2)	77/female	Dysphasia	No	Euthyroid	Postoperative pathological examination	Proximal esophagus	DLBCL	IIE	Surgical excision, chemotherapy	CR on the CT images
	73/female	Voice change	No	Euthyroid	Postoperative pathological examination	Tracheal, laryngeal, and esophageal invasion	DLBCL	IE	Surgical excision, chemotherapy	CR on the CT images
Hu *et al.* (3)	63/female	A rapidly growing mass in the front of her neck	No	Euthyroid	Postoperative pathological examination	RIJV and adjacent muscles	DLBCL	IE	Surgical excision, chemotherapy	NA
	60/male	A rapidly enlarged thyroid and several nodules in the front of his neck	No	Hypothyroid	FNAB	Adjacent muscles in the front of his neck	DLBCL	IIE	Chemotherapy	NA
Chen *et al.* (4)	80/female	Diffuse enlargement of the thyroid gland and a left sided neck mass	No	NA	FNAB	Tracheal	DLBCL	IE	Chemotherapy	NA
Su (this study)	79/female	Neck mass with pain	Yes	Hyperthyroid	FNAB, CNB	RIJV	DLBCL	IIE	Chemotherapy	CR on the CT images
	89/female	Neck mass	Yes	Euthyroid	FNAB, CNB	LIJV carcinoma thrombosis	DLBCL	IIE	Observation	NA
	79/male	Neck mass	Yes	Euthyroid	FNAB, CNB	Encapsulated right common carotid artery, RIJV carcinoma thrombosis	DLBCL	IE	Chemotherapy	CR on the CT images

PTL, primary thyroid lymphoma; HT, Hashimoto's thyroiditis; DLBCL, diffuse large B-cell lymphoma; CR, complete remission; CT; computed tomography; RIJV, right internal jugular vein; NA, not available; FNAB, fine-needle aspiration biopsy; CNB, core needle biopsy; LIJV, left internal jugular vein.

cases, the contrast agent entered in a centripetal way and presented with hypo-enhancement and heterogeneity. This is similar to the enhancement characteristics of malignant thyroid lesions reported in the existing literature. All 3 cases received FNAB and/or CNB for thyroid masses, and pathology was confirmed as DLBCL. This is consistent with the previous literature on lymphomas that invade peripheral tissues related to the type of pathology, both of which are DLBCL. The enhancement characteristics of the IJV emboli of cases were different after contrast agent injection. This may be related to the cause and stage of tumor thrombus formation. The mechanism of tumor thrombus formation is not well understood and requires observations and summaries of more cases. We performed FNAB on the RIJV embolus in case 3 under US guidance, and a very small amount of atypical lymphoid cells were found under the pathological microscope. This is the first report of PTL invading the IJV in which a tumor thrombus formed, which was confirmed by an ultrasound-guided pathological puncture.

Aggressive PTL can invade inside the lumen of the IJV, and cases 1 and 3 in this study achieved CR after regular chemotherapy. This suggests that regular chemotherapy is still effective in treating aggressive PTL that invades the IJV. US-guided FNAB and/or CNB were performed on the neck mass in the 3 patients, and we performed the associated pathological diagnosis using the puncture sample to avoid diagnostic surgery. In addition, we performed FNAB on the IJV thrombus in case 3 and confirmed it to be a tumor thrombus, which clarified the extent of PTL invasion.

US and CEUS can be used to diagnose PTL and can also be used to assess the invasion of PTL to surrounding tissues, lymph nodes, and vessels in the neck. US-guided FNAB and CNB for neck masses in 3 cases and FNAB for IJV emboli incurred no serious complications, which avoids the risks and complications associated with diagnostic surgery. Regular chemotherapy is still effective for aggressive PTL invading the IJV to form tumor thrombus, which can avoid IJV removal or embolectomy. Among the invading IJV disease, PTL should also be considered in clinical diagnosis and treatment. The rational use of US, CEUS, FNA, and CNB is helpful for the early diagnosis of PTL and guidance for subsequent treatment.

Acknowledgments

Funding: None.

Footnote

Conflicts of Interest: All authors have completed the ICMJE uniform disclosure form (available at https://qims.amegroups.com/article/view/10.21037/qims-22-649/coif). The authors have no conflicts of interest to declare.

Ethical Statement: The authors are accountable for all aspects of the work in ensuring that questions related to the accuracy or integrity of any part of the work are appropriately investigated and resolved. All procedures performed in this study were in accordance with the ethical standards of the institutional and/or national research committee(s) and with the Helsinki Declaration (as revised in 2013). Written informed consent was provided by the patient for the publication of this case report and accompanying images. A copy of the written consent is available for review by the editorial office of this journal.

References

1. Stein SA, Wartofsky L. Primary thyroid lymphoma: a clinical review. J Clin Endocrinol Metab 2013;98:3131-8.
2. Kim EH, Kim JY, Kim TJ. Aggressive primary thyroid lymphoma: imaging features of two elderly patients. Ultrasonography 2014;33:298-302.
3. Hu G, Zhu X. Ultrasonographic features of aggressive primary thyroid diffuse B-cell lymphoma: A report of two cases. Oncol Lett 2016;11:2487-90.
4. Chen C, Tibbetts KM, Tassler AB, et al. Tracheal invasion and perforation from advanced primary thyroid lymphoma: a case report and literature review. Am J Otolaryngol 2013;34:559-62.
5. Adler DD, Carson PL, Rubin JM, et al. Doppler ultrasound color flow imaging in the study of breast cancer: preliminary findings. Ultrasound Med Biol 1990;16:553-9.
6. Tessler FN, Middleton WD, Grant EG, et al. ACR

Thyroid Imaging, Reporting and Data System (TI-RADS): White Paper of the ACR TI-RADS Committee. J Am Coll Radiol 2017;14:587-95.
7. Sun TQ, Zhu XL, Wang ZY, et al. Characteristics and prognosis of primary thyroid non-Hodgkin's lymphoma in Chinese patients. J Surg Oncol 2010;101:545-50.
8. Nam M, Shin JH, Han BK, et al. Thyroid lymphoma: correlation of radiologic and pathologic features. J Ultrasound Med 2012;31:589-94.
9. Greis C. Quantitative evaluation of microvascular blood flow by contrast-enhanced ultrasound (CEUS). Clin Hemorheol Microcirc 2011;49:137-49.
10. Radzina M, Ratniece M, Putrins DS, et al. Performance of Contrast-Enhanced Ultrasound in Thyroid Nodules: Review of Current State and Future Perspectives. Cancers (Basel) 2021;13:5469.
11. Zhang Y, Luo YK, Zhang MB, et al. Diagnostic Accuracy of Contrast-Enhanced Ultrasound Enhancement Patterns for Thyroid Nodules. Med Sci Monit 2016;22:4755-64.
12. Wu Q, Wang Y, Li Y, et al. Diagnostic value of contrast-enhanced ultrasound in solid thyroid nodules with and without enhancement. Endocrine 2016;53:480-8.
13. Ma X, Zhang B, Ling W, et al. Contrast-enhanced sonography for the identification of benign and malignant thyroid nodules: Systematic review and meta-analysis. J Clin Ultrasound 2016;44:199-209.
14. Yang L, Zhao H, He Y, et al. Contrast-Enhanced Ultrasound in the Differential Diagnosis of Primary Thyroid Lymphoma and Nodular Hashimoto's Thyroiditis in a Background of Heterogeneous Parenchyma. Front Oncol 2021;10:597975.
15. Tarantino L, Ambrosino P, Di Minno MN. Contrast-enhanced ultrasound in differentiating malignant from benign portal vein thrombosis in hepatocellular carcinoma. World J Gastroenterol 2015;21:9457-60.
16. Li Q, Wang Z, Ma X, et al. Diagnostic accuracy of contrast-enhanced ultrasound for detecting bland thrombus from inferior vena cava tumor thrombus in patients with renal cell carcinoma. Int Braz J Urol 2020;46:92-100.
17. Trimboli P, Crescenzi A. Thyroid core needle biopsy: taking stock of the situation. Endocrine 2015;48:779-85.
18. Zhang L, Castellana M, Virili C, et al. Fine-needle aspiration to diagnose primary thyroid lymphomas: a systematic review and meta-analysis. Eur J Endocrinol 2019;180:177-87.
19. Huang CG, Li MZ, Wang SH, et al. The diagnosis of primary thyroid lymphoma by fine-needle aspiration, cell block, and immunohistochemistry technique. Diagn Cytopathol 2020;48:1041-7.
20. Pavlidis ET, Pavlidis TE. A Review of Primary Thyroid Lymphoma: Molecular Factors, Diagnosis and Management. J Invest Surg 2019;32:137-42.

Cite this article as: Su X, Hu X, Ma B. Aggressive primary thyroid lymphoma invading the internal jugular vein: a case series. Quant Imaging Med Surg 2023;13(2):1213-1220. doi: 10.21037/qims-22-649

